INTERNATIONAL ATOMIC ENERGY AGENCY
UNITED NATIONS EDUCATIONAL, SCIENTIFIC AND CULTURAL ORGANIZATION

INTERNATIONAL CENTRE FOR THEORETICAL PHYSICS
34100 TRIESTE (ITALY) - P.O.B. 586 - MIRAMARE - STRADA COSTIERA 11 - TELEPHONES: 224281/2/3/4/5/6
CABLE: CENTRATOM - TELEX 460392-1

SMR/113 - 14

AUTUMN COLLEGE

ON

THE TROPOSPHERE, STRATOSPHERE AND MESOSPHERE

10 September - 19 October 1984

NUMERICAL MODEL

Lectures 1 - 5

P.K. DAS

Department of Meteorology
University of Nairobi
P.O. Box 30197
Nairobi
Kenya

LECTURE III

BAROTROPIC AND BAROCLINIC INSTABILITY

The origin of waves and similar disturbances is often attributed to instability in the atmosphere. Two types of instability have been invoked.

The first leads to the conversion of potential energy to the kinetic energy of motion. Although the atmosphere has a large store of potential energy, only a small fraction is available for conversion to kinetic energy (KE). This was named the Available Potential Energy (APE) by Lorenz (1955). It represents the surplus of potential energy from a hypothetical state in which no further conversion of potential energy is possible. The lines of constant entropy (isentropes) and pressure (isobars) coincide in this hypothetical state.

Conversion of APE to KE is the outcome of a form of instability which is referred to as baroclinic instability. Vertical wind shears dominate a baroclinic atmosphere. Baroclinic instability is illustrated by the following situation.

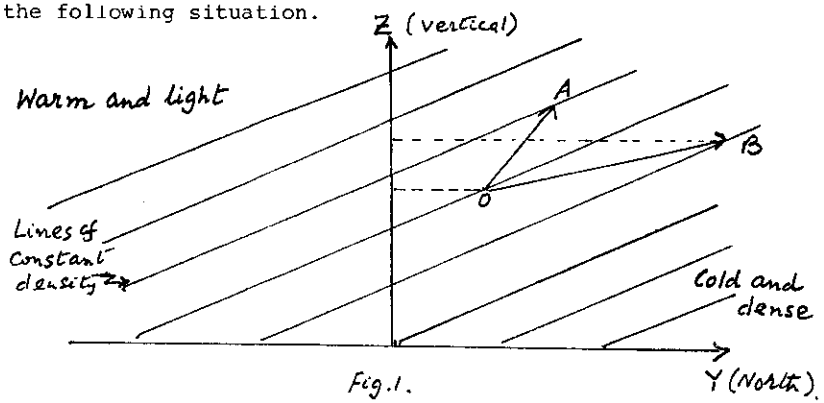

Fig.1.
Baroclinic Instability.

We imagine a situation in which lines of constant density slope in a north-south direction, such that colder (denser air) lies to the north. The density also decreases with height. Consider a particle at O to move to A without interacting with the environment. As the particle at O comes from a denser region, it will be colder than its environment and will tend to sink back to its original location. Similarly, if A moves to O it will be warmer than its environment and will experience a restoring force upwards. But, if O is moved to a new location B, which is higher than O and is more dense; the force of buoyancy will tend to separate A and B further, and eventually lead to instability. As we can see, this type of instability is determined by the slope of lines of equal density (or entropy). In physical terms, the north-south slope of density lines implies a horizontal temperature gradient, or a vertical wind shear through a thermal wind.

Another form of instability in the atmosphere does not convert APE to KE, but transfers KE from an atmosphere lying in a state of equilibrium to motion on a smaller scale. A meteorological wave, which we imagine to be superposed on a mean state of equilibrium, may thus derive its energy from the mean state. Instability of this kind, which redistributes the kinetic energy of the atmosphere, is known as barotropic instability. Barotropic instability is the outcome of horizontal wind shear.

But, both vertical and horizontal wind shears exist in the real atmosphere. Consequently, it is more realistic to consider combined baroclinic and barotropic instability.

The instability of sheared flow in the atmosphere leads to a spectrum of fluctuations or perturbations. A meteorologist has two obj-ctives: he seeks to determine conditions which lead to instability and, secondly, to identify the scale and period of perturbations which grow fastest with time. The fastest growing perturbation is believed to represent a preferred scale of motion. If the dimensions of tropospheric waves over Africa, for example, agree with the length and time scales of the dominant mode, then it is inferred that these waves are the outcome of barotropic or baroclinic instability, as the case may be.

Unstable baroclinic perturbations tend to transfer heat from warmer to colder regions so as to stabilize the atmosphere. The transfer of heat is down the gradient of temperature. Similarly, barotropic perturbations transfer momentum down the momentum gradient. A difficulty arises here: imagine a perturbation, being baroclinically unstable, drawing upon the APE of the mean state, but at the same time it generates additional Reynolds stresses which feed momentum back to the mean state. To be unstable, a perturbation should extract more energy than it returns. The ability of transfer mechanisms to proceed in both directions is determined by the inclination of a wave-like perturbation with

respect to height and latitude.

2. NECESSARY CONDITIONS

(a) Barotropic instability

Several necessary conditions have been established for barotropic instability. It is worthwhile to emphasize that the conditions are necessary; it has not been possible to establish that they are sufficient by themselves, except in a few cases.

A widely used condition requires the existence of a point where the profile of absolute vorticity changes sign within the region of interest. If it is assumed that the mean state of the atmosphere is a current of air $U(y)$, whose strength varies with y, then the existence of barotropic instability implies that at some point in the region $\left(\beta - \frac{d^2U}{dy^2}\right)$ should vanish. This necessary condition was originally derived by Lord Rayleigh in 1880, but was later modified by Kuo to include the earth's rotation. Of the other necessary conditions, a theorem by Fjortoft (1950) asserts that the mean speed $U(y)$ at the point of inflection should not be exceeded at any other point in the region.

(b) Baroclinic instability.

Two celebrated papers; one by Charney (1947) followed shortly later by Eady (1949) formed the basis of subsequent research. Unfortunately, it is very difficult to establish the conditions for instability for a perfectly general case. Eady's model is simpler,

but he assumed a rigid lid at the top of the atmosphere and no internal gradient of potential vorticity within the fluid. The analysis was further simplified by assuming a constant value of the Coriolis parameter (f).

On introducing these simplifications, Eady's model suggests that perturbations will amplify if

$$k^2 + l^2 < 5.76 \frac{f^2}{N^2 H^2} \qquad (2.1)$$

where k and l represent wave numbers in the zonal (ox) and meridional (oy) directions. If typical values are inserted for the tropics, that is, if $f = 5 \times 10^{-5}\ s^{-1}$, $N^2 = 10^{-4}\ s^{-2}$ and H = 10 km, then amplifying waves are only possible, if the wave length exceeds 7000 km. The growth rate of such long waves is small. But, Pearce (1981) found that enhanced growth rates for shorter waves were possible if β, the meridional gradient of f, is included in the Eady model. This is an interesting result for the summer monsoon, because the wind field reverses its direction in the middle troposphere. The winds in the lower troposphere are westerly, while they become easterly in the upper troposphere. Eady's model would preclude the growth of transient disturbances, such as depressions in the monsoon regime, unless the shorter waves were destabilised by the inclusion of beta. Charney's model is more difficult to interpret, but it suggests that for a vertical shear of 2 m s^{-1}/km, the wave length of maximum instability is about 5000 km, and the amplitude

doubles in 2 days. This agrees with the results of Eady's model.

The classical papers of Charney and Eady have been followed by a large number of research publications, which have had an important bearing on the subsequent development of numerical models. The theory has been largely confined so far to linear equations. An extension to non-linear systems by expansion in terms of a small parameter would be interesting for possible applications in the tropics.

(c) Combined barotropic-baroclinic instability.

A brief definition of potential vorticity was provided earlier. The definition may be expanded by combining the equations for conservation of vorticity and entropy for quasi-geostrophic motion, without any external forcing. This provides us with the conservation of another variable which is known as the potential vorticity (q). We have

$$\frac{Dq}{Dt} = 0 \qquad (2.1)$$

where

$$q = \zeta + f + f_0^2 \frac{\partial}{\partial p}\left(\frac{1}{N^2}\frac{\partial \psi}{\partial p}\right) \qquad (2.2)$$

and ψ is a stream function.

When combined barotropic-baroclinic instability is considered, Charney and Stern (1962) derived a necessary condition which was similar to the inflection point theorem of Rayleigh and Kuo. But, instead of the absolute vorticity profile, the relevant parameter was potential vorticity. The condition stipulates that $\frac{\partial \bar{q}}{\partial y}$ must vanish at some point in the region of

interest.

3. Practical applications

Despite considerable theoretical work on instability, the results have not been conclusive. It has been observed, for example, that considerable divergences of opinion arise. A search for inflection points, in the profile of absolute vorticity or potential vorticity, reveals a multiplicity of such points, not all of which are associated with waves.

Similar divergences arise in the scale of dominant modes. Over Africa, for example, observations suggest the westward propagation of waves, which are believed to be the precursors of tropical cyclones in the Atlantic. Large horizontal wind shears associated with a mid-tropospheric jet stream leads to a vorticity profile that favours barotropic instability over eastern Africa, and baroclinic or combined barotropic-baroclinic instability over central and western Africa. Satellite observations and observational data suggest that these waves have a wavelength of about 2500 km, and a phase speed of 5 m S^{-1}. One disturbance moves westward every 3 to 4 days over a station. But, there appears divergence in the results of instability theory to explain the fastest growing disturbances (Table 1).

Table 1

Instability of fastest growing disturbances.

	Wavelength (km)	Growth rate (day^{-1})	Phase speed (mS^{-1})
Rennick (1976-1981)	2800-5300	0.04 to 0.44	15.8
Simmons (1977)	3900	0.27	8-9
Mass (1979)	2500	0.52	7.5

Similar divergences appear when instability theory is invoked to explain the formation of monsoon depressions in the Bay of Bengal, for example; or the onset of the summer monsoon over the southern part of the Indian Peninsula.

A peculiar feature appears when attempts are made to include atmospheric convection in instability analysis. Nortmally, one would expect warming by latent heat release would add to the APE of the atmosphere and increase the rate of conversion to K.E. But, the few attempts to do this for African waves suggest no major change in the characteristics of the dominant wave. An attempt to parameterize latent heat release in clouds for monsoon depressions leads one to conclude that the dominant mode is not the one that grows fastest, but the one that reaches

equilibrium fastest with the environment (Shukla, 1978). The present picture is unclear, and casts doubt on the capability of linear models to explain the growth of unstable modes when other forcing mechanisms, apart from wind shear, are considered.

4. Vertical propagation of energy.

Most of the kinetic energy of the atmosphere, and about 80% of its mass resides in the troposphere. It is interesting to investigate the possibility of some of the energy propagating into the lower stratosphere.

Mention has been made of the vertical structure of equatorial waves and a critical value of the equivalent depth for vertical propagation to take place, but the analysis did not contain a variable mean wind or the atmospheric response to tropospheric forcing. These aspects were investigated by Charney and Drazin in 1961. Briefly stated, Charney and Drazin's result indicates that if U, the zonal current, and N, the Brunt-Vaisala frequency, are slowly varying functions of the altitude (Z), the amplitude equation for free waves, determines the vertical propagation of energy by a refractive index (n), because the solutions of the equation behave as $\exp(inz/2)$

It follows then that, roughly speaking,

$n^2/4 > 0$: Oscillatory solutions which

$n^2/4 < 0$: Solutions damped with Z, and energy propagation inhibited.

The refractive index is a function of the zonal current (U), beta, the static stability (N) and an average value of the Coriolis parameter (f_o).

Computations of the refractive index (n) from observed profiles of U and N^2 between 30° and 60° for different values of wavelength show that the waves are strongly trapped in the summer stratosphere above 20 km because of large negative values of n. A similar situation also prevails in winter for shorter waves. Only during the equinoxes, does there appear possibility of propagation to high altitudes.

The trapping of waves by an easterly wind (negative U) has been suggested as a possible reason to explain why the waves in the lower equatorial troposphere are decoupled with the westerly winds of the upper troposphere.

An extension of this analysis to a zonal current, which also varies in a meridional direction ($U(y,z)$) by Dickinson (1969) has led to the inference that similar trapping of equatorial disturbances is possible at a critical latitude. This suggests that the tropics are again decoupled from the mid-latitudes.

Opinion is still divided on this question because model experiments indicate that mid-latitude systems can, on few occasions, move into lower latitudes and vice versa. The analysis is based on a zonal current $U(y,z)$ which is assumed to be reasonably steady, and non-linear interactions have been ignored. Both these assumptions are questionable in a real atmosphere.

REFERENCES

Charney, J.G. 1947 The dynamics of long waves in a baroclinic westerly current, J. Meteor., U.S.A., 4, 135-162.

——— and M. Stern 1962 On the stability of internal baroclinic jets in a rotating atmosphere, J. Atmos. Sci., 19, 159-172.

Eady, E.J. 1949 Long waves and cyclone waves, Tellus, 1, 3, 33-52.

Fjortoft, R., 1950 Application of integral theorems for stability, Geophysik. Publn., Osio, 17, 5-52.

Lorenz, E.N. 1955 Available potential enery and maintenance of the general circulation, Tellics, Telluss 7, 157-167.

Mass, C. 1979 A linear primitive equation model for African waves, J. Atmos. Sci., 36, 2075-2092.

(Contd.)

Rennick, M.A. 1976 The generation of African waves, J. Atmos. Sci. 33, 1955-1969.

Rennick, M.A. 1981 Some Sensitivity experiments with African waves, JI J. Atmos. Sci., 38, 106-114.

Shukla, J. 1978 CISK, barotropic-baroclinic instability and growth of a monsoon depression, J. Atmos. Sci., 35, 495-508.

Simmons, A.J. 1977 The instability of African easterly jet, J. Atmos. Sci., 34, 1670-1674.

LECTURE II

1. METEOROLOGICAL NOISE

Mention was made in the last lecture how Richardson's computation led to an unreaslistic pressure change of 145 mb in 6 hours for a station in Central Europe. The observed pressure change was only a fraction of a mb in the same time interval.

The reason for this peculiar result was not discovered till another 25 years had elapsed. The basic equations, which were discussed in the first lecture, support a wide variety of waves in the atmosphere. Some are fast moving and highly dispersive, such as, sound waves and inertia-gravity waves. But, there exist another class of waves, which move westwards with slower speed and are much less dispersive. Their speed of propagation agrees well with what is observed on weather charts in mid-latitudes. They are known as Rossby waves after the Swedish meteorologist, C.G. Rossby. Charney (1947 , 1948) showed that it was necessary to filter out the faster modes before commencing integration of the relevant equations; otherwise, the faster modes soon begin to dominate and create wide fluctuations in the numerical solution. Briefly stated, this was the reason why Richardson found large changes in pressure.

Charney's second important contribution was to show that the faster waves could be suppressed by two constraints on the initial state of the atmosphere. First, the

assumption of hydrostatic equilibrium excluded sound waves. Second, the geostrophic assumption removed inertia-gravity waves.

But, subsequent work by Matsuno (1966) indicates that, in low latitudes, a class of solutions exists which has the characteristics of both Rossby and inertia-gravity waves. This precludes the possibility of separating the Rossby and faster moving waves. But, let us first see how the Rossby waves are separated from the others.

2. SEPARATION OF ROSSBY MODES.

Let us consider a stratified atmosphere at rest with $\bar{T} = \bar{T}(p)$, $\frac{d\bar{\phi}}{dp} = -\frac{R\bar{T}}{p}$ and $\Gamma(p) = -\frac{1}{\bar{\theta}}\frac{\partial}{\partial p}\ln\bar{\theta}$.

A bar denotes a mean value.

If perturbations of small amplitude are imposed on this ideal atmosphere, the linear perturbation equations are

$$\frac{\partial u'}{\partial t} - fv' = -\frac{\partial \phi'}{\partial x} \qquad (2.1)$$

$$\frac{\partial v'}{\partial t} + fu' = -\frac{\partial \phi'}{\partial y} \qquad (2.2)$$

$$\frac{\partial \omega'}{\partial p} + \left(\frac{\partial u'}{\partial x} + \frac{\partial v'}{\partial y}\right) = 0 \qquad (2.3)$$

$$\frac{\partial}{\partial t}\left(\frac{\partial \phi'}{\partial p}\right) + \Gamma(p)\,\omega' = 0 \qquad (2.4)$$

where u', v', ω' are the components of perturbed motion and the other quatities have been defined before.

Solutions of the above set of equations may be derived by separating variables. The theory of tidal motion show that the separation constant (c^2) has the dimensions of the square of velocity. It is often expressed as the

product of g and the height of a homogeneous ocean (h_n). The subscript n denotes the eigenvalues for the vertical structure.

Let us first consider the vertical structure of the disturbance. Without going into the mathematical details, it can be shown (Phillips, 1973) that two classes of waves emerge:

(i) c equals the speed of sound.

The perturbations decrease in amplitude with altitude. The vertical velocity (ω'), for example, decreases with pressure as $(p/p_0)^{1/\gamma}$, where $\gamma = c_p/c_v$. This is known as the Lamb wave. The Lamb waves is an external mode of oscillation.

(ii) c^2 varies from o to ∞ in the form of a continuous spectrum.

The perturbations now have a sinusoidal vertical structure, such as, $\sin mz$ or $\cos mz$, where m is a real number whose value ranges from 0 to ∞.
For short vertical wavelengths $m \to \infty$ and $c \to 0$, while for large wavelengths $m \to 0$ and c approaches the velocity of sound.

To determine the horizontal structure, we assume that each perturbation has the form

$$F(y) \times \exp(is\lambda) \times \exp(-i\omega t) \qquad (2.5)$$

where s is a zonal wave number, λ stands for longitude and ω is the frequency. F(y) is the meridional structure of perturbations. Assuming that the perturbations vanish at the poles, and using (2.5) in the linear perturbation

equations, we get a differential equation for F(y), whose solutions determine the frequencies of permissible waves. Three types of wave motion emerge, whose frequencies are:

$$\omega_1 = [f^2 + c^2(k^2+l^2)]^{1/2} \qquad (2.6)$$

$$\omega_2 = -\omega_1 \qquad (2.7)$$

$$\omega_3 = -\beta k/[(k^2+l^2) + f^2/c^2] \qquad (2.8)$$

where k, l are zonal and meridional wave numbers.

The first two are referred to as inertia-gravity waves. Their frequency is about 9 cycles/day. The last one is known as a Rossby wave. Its frequency is only 0.07 cycle/day, which is much smaller than the other two. For typical values of c ($300 ms^{-1}$), $\frac{f^2}{c^2}$ is an order of magnitude smaller than $(k^2 + l^2)$, consequently,

$$\omega_3 \simeq -\beta k/(k^2+l^2) \qquad (2.9)$$

The phase velocity (c_p) of Rossby waves is readily derived as

$$c_{pR} = \frac{\omega}{(k^2+l^2)^{1/2}} \simeq \frac{-\beta k}{(k^2+l^2)^{3/2}} \qquad (2.10)$$

The dispersion of Rossby waves is measured by its group velocity cg_x in the x direction.

We have

$$c_{gx} = \frac{\partial \omega}{\partial k} = \frac{\beta(k^2-l^2)}{(k^2+l^2)^2} \qquad (2.11)$$

In mid-latitudes, if we consider a wavelength of 4000km, the phase velocity (c_{ph}) is about 2.5 ms^{-1}. The negative sign before (2.10) indicates that Rossby waves move westwards. Comparing (2.11) with (2.10), it is interesting to note that while the phase velocity is always to the west, the group velocity could be to the

east or west depending on whether k is greater or less than 1. On mid-latitude weather charts, it is observed that large scale waves move from west to east. This might appear to contradict Rossby waves which move in the opposite direction. The apparent contradiction is avoided if we consider Rossby waves are superposed on a zonal current, which is directed eastwards with a speed of $10ms^{-1}$. The speed is much greater than the phase speed of Rossby waves.

3. WAVES IN THE EQUATORIAL ATMOSPHERE

During the past decade there has been an upsurge of interest in the dynamics of equatorial waves because of the realization that Laplace's tidal equation yields interesting solutions near the equator. A survey of tropical waves is available in a publication by Beer (1978). An attempt here will be to attempt a summary of the main features.

The equatorial beta plane approximation which was described in the previous lecture, was used by Matsuno (1966) to derive the horizontal structure of equatorial waves from shallow water equations. This system of equations is valid for waves whose wavelengths are much greater than the depth of the fluid. This restriction is necessary for the hydrostatic approximation to be valid.

Matsuno found that, in addition to eastward and westward propagating inertia-gravity waves and a westward

Rossby wave, two other modes were possible:

(a) The first mode displayed the features of Rossby waves for small wave numbers, but resembled inertia-gravity waves for larger wave numbers. Both were trapped near the equator. This is now referred to as a mixed Rossby-gravity wave, or a Yanai wave.

(b) The second is called an equatorial kelvin wave, This is an eastward moving wave in which the zonal velocity and meridional pressure fields are in exact balance, so that there is no meridional component of velocity. Kelvin waves have periods in the range of 12-20 days and a wave-length which spans the earth's circumstance.

These unbounded modes can be expressed mathematically in terms of Hermite polynomials $(H_n(y))$. The three categories of waves, which we have just mentioned, may be described by the value of n. Thus,

(i) $n \geq 1$ modes: Two classes of waves, which are separable. The represent inertia-gravity and Rossby modes.

(ii) $n = 0$: Yanai or mixed Rossby gravity wave.

(iii) $n = -1$: Equatorial Kelvin wave.

The vertical structure of equatorial waves was derived by Lindzen (1967). Defining the vertical wave number by

$$\lambda = \left(\frac{\Gamma}{gh_n} - \frac{1}{4}\right)^{1/2} \qquad (3.1)$$

where Γ is the static stability parameter defined earlier, and h_n represents an equivalent depth, Lindzen concluded that the vertical propagation of a wave depended

on the equivalent depth and the static stability of the atmosphere. He suggests:

(a) $0 < h_n < \frac{4\Gamma}{g}$: Vertical propagation permissible

(b) $h_n > \frac{4\Gamma}{g}$: Waves vertically trapped.

or $h < 0$

The critical value of $h_n = \frac{4\Gamma}{g}$ is about 8.6km. This will increase as the static stability increases. The horizontal structure equation or the vertical structure equation should have a forcing term. In the atmosphere the nature of forcing is generally in the vertical direction, while in the oceans it is in the horizontal direction. The need to include forcing arises, if we wish to find out how the upper atmosphere responds to tropospheric forcing by generating free waves that might resonate with the atmopshere, or forced waves that propagate away from the source. For an isothermal atmosphere, in hydrostatic balance the only possibility of a free wave resonating with the atmosphere is a lamb wave.

Several conjectures have appeared in recent years to suggest that monsoonal circulations might generate a response in the upper atmosphere, especially the lower stratosphere. The warming of the atmosphere by the release of latent heat in cumulus clouds, especially in the tropics, has been also suggested as a possible source of excitation. These conjectures have not yet been tested in a quantitative manner by model experiments, although an experiment performed twenty years ago did suggest an average monthly warming of 3.2°c/day over some parts of the

summer monsoon.

Although there exists some uncertainty on the source of excitation, a considerable volume of evidence is beginning to appear on wave motion and periodicities, notwithstanding difficulties in interpretation. The principal tools for detecting waves are:

- Time series of radiosonde data
- Compositing a number of wind fluctuations
- Satellite and radar tracking of cloud clusters.

The diverse waves and periodicities are summarised in table 1.

Table 1

ATMOSPHERIC WAVES AND PERIODICITIES

	1	2	3	4
	Period (days)	L_x (km)	L_z (km)	Observations
1.	2	2000	-	Wind spectra at Ascension Island (8°s, 10 w)
2.	4-5	4000	6	Believed to be mixed Rossby-gravity modes in stratosphere.
3.	4-5	4000	6	Horizontal waves observed over central and W. Africa and E. Pacific Ocean.
4.	10-15	30,000	6-8	Believed to be a Kelvin

Table 1

ATMOSPHERIC WAVES AND PERIODICITIES (ctd..)

	1 Period (days)	2 L_x (km)	3 L_z (km)	4 Observations
4.	10-15	30,000	6-8	wave in lower stratosphere, (18-25 km). Strong eastweard modes near 25km. evidence of waves in lower troposphere but moving westward, 15 day oscillation claimed for summer monsoon rain over India.
5.	15-25	30,000	6-8	Satellite observed cloudiness. Appears to be similar to Kelvin wave.
6.	40-50	-	-	Oscillation observed at Canton Island in the Pacific, Associated with an east-west oriented Walker cell.

L_x = horizontal wave length.

L_z = vertical wave length.

In addition to the periodicities mentioned in table 1, evidence has been adduced for a semiannual and a quasi-biennial oscillation. We will not discuss these two oscillations because they are beyond the scope of this lecture. But, while the semiannual oscillation, which is observed in the equatorial stratosphere, appears to be forced from below because of downward phase propagation, the quasi-bienniel oscillation appears to be an outcome of interactions between vertically propagating internal waves and lower stratospheric winds.

Literature on the waves mentioned in Table 1 is very extensive, and it will be hardly possible to provide a complete review. A review article by Beer (1978) provides a comprehensive list of references upto 1978. Some of the prominent articles that have appeared subsequently are:

(i) African Waves : Njau (1982), Thompson et al (1979).

(ii) 40-50 day Cycle : Krishnamurti and D. Subrahmanyam (1982), Yasunari (1981), Lorenc (1984).

It would be appropriate to conclude this lecture with a word of caution. While it is clearly not our intention to denigrate the attempts to search for atmospheric signals, on different scales of length and time, one needs to proceed cautiously against premature inferences, The periodicities discovered so far have not had the impact on weather prediction, which their discovery might warrant. The search is likely to continue until more definite results emerge.

REFERENCES

Beer, T. 1978 Tropical Waves, Rev. Geophys & Space Sc., 6, 4, 567-581.

Charney, J.G. 1948 On the scale of atmospheric motions, Geophys. publick, 17, 17 pp.

Krishnamurti, T.N. and D.Subrahmanyam 1982 The 30-50 day mode at 850 mb during MONEX, J. Atmos. Sci., 39, 2088-2095.

Lindzen, R.S. 1967- Planetary waves on beta planes, Mon. Wea. Rev., 95, 441-451.

Lorenc, A.C. 1984 The evolution of planetary scale 200 mb divergent flow during the FGGE year, Quat. J. Roy. Met. Soc., 110, 464, 427-442.

Matsuno, T. 1966 Quasi-geostrophic motions in the equatorial area, J.Met. Soc., Japan, 44, 25-43.

Njau, L.N. 1982 Tropospheric Wave disturbances in E. Africa, M.Sc. Thesis (unpublished), Univ. of Nairobi, 161 pp.

REFERENCES (CONTD..)

Phillips, N.A. 1973 Principles of large Scale numerical weazher prediction, Dynamic Meteorology, Ed. P. Morel, D. Reidel Publishing Co., 1-96, pp.

Thompson, R.M. S.W. Payne, E.E.Recker and R.J.Read. 1979 Structure and properties of synoptic scale wave disturbances in the intertropical convergence zone of the E.A. Atlantic, J. Atmos. Sci, 36, 53-72.

Yasumari, T. 1981 Structure of an Indian summer monson system with around 40 day period, J. Met. Soc. Japan, 59, 336-354.

MESOSPHERE, STRATOSPHERE AND TROPOSPHERE

NUMERICAL MODELS

By

P.K. Das, University of Nairobi, Kenya.

LECTURE I.

1. INTRODUCTION

I wish to begin by expressing my gratitude to the organizers of this course.

It is a privilege to speak before this distinguished audience, and to visit a centre which has done so much to encourage the growth of science in the developing world.

Rapid strides have taken place in the design of numerical models. It will be hardly possible to cover all facets; consequently, my attempt will be to present those physical ideas on which there has been considerable research in recent years. Mathematical details will be eschewed as far as possible, but references will be provided to original papers where the interested reader could find them.

2. HISTORICAL DEVELOPMENT

The historical development of weather prediction, especially numerical weather prediction, may be traced with reference to several milestones. Briefly stated, the important landmarks up to 1950 are:

A.D. (ca)

1643 : Discovery of the barometer by Torricelli

1820 : Appearance of first weather chart with old data.

1845 : Discovery of Telegraph and Improved data collection.

1904 : V. Bjerknes suggested weather prediction as an initial value problem.

1920 : First attempt at numerical prediction by L.F. Richardson. Computed pressure change at a station in Central Europe was 145mb/6 hours.

1945 : Electronic computers emerge.

1950 : First weather forecast prepared on ENIAC (Electronic Numerical integrator and calculator) by Von Neumann, J.G. Charney and R.Fjortoft.

3. BASIC EQUATIONS

The equations that govern atmospheric motion may be traced back to Laplace's theory of tides (1799-1823). Laplace was interested in oscillations of an ocean of uniform depth on a rotating earth, which was gravitationally forced.

The basic equations express the conservation of momentum, mass and entropy for an atmosphere in motion. If we add the gas law for air, and assume hydrostatic balance, then a system is obtained in which the number of equations equals the number of unknowns. This can be integrated, if sufficient computing power is available and the initial and boundary conditions are specified with adequate accuracy. The systems is highly non-linear.

For a reference frame rotating with the earth, the conservation of momentum is expressed by

$$\frac{D\vec{V}}{Dt} + 2\vec{\Omega}\times\vec{V} = -\frac{1}{\rho}\nabla p + g\vec{k} + \vec{F} \qquad (2.1)$$

where $\vec{V}$ is the velocity relative to a rotating earth, $\vec{\Omega}$ stands for the earths rotation vector ($|\Omega| = 7.29\times10^{-5}\,s^{-1}$), ρ is the density of air, p is pressure and g stands for

acceleration due to gravity. Friction and other body forces are represented by $\vec{F}$. Equation (2.1) may be expressed in cartesian or spherical coordinates. For simplicity, cartesian coordinates (oxyz) are usually used with ox pointing east, oy points northwards and oz is the vertical axis of reference. The constant g is the sum of gravitation and a small centrifugal force due to the earth's rotation ($\vec{\Omega} \times \vec{\Omega} \times \vec{r}$) for a particle at a distance $\vec{r}$ from the earth's centre. This ignores the ellipticity of the earth, but the error is small. Although cartesian coordinates are most widely used, we will see later that it is sometimes more convenient to use spherical coordinates. For meteorological models, it is also more convenient to use pressure, or some function of pressure, as the vertical coordinate instead of altitude (z). This will be discussed later.

The total derivative following the motion is the sum of a local and an advective change. We put

$$\frac{D}{Dt} \equiv \frac{\partial}{\partial t} + \vec{V} \cdot \nabla \qquad (2.2)$$

The second term on the left of (2.1) measures the effect of the earth's rotation ($2\vec{\Omega} \times \vec{V}$). It is known as the Coriolis force after G. Coriolis, the scientist who discovered its existence. It is to be noted that the earth's rotation vector has the dimensions of a frequency (s^{-1}). For this reason, it may be referred to as a Coriolis frequency.

When the motion is under hydrostatic balance, (2.1) is equivalent to

$$\frac{D\vec{V}_h}{Dt} + \vec{f} \times \vec{V}_h = -\frac{1}{\rho} \nabla p + \vec{F}_h \qquad (2.3)$$

and

$$\frac{\partial p}{\partial z} = -g\rho \qquad (2.4)$$

where $\vec{V}_h$ is the horizontal wind velocity, $\vec{F}_h$ is the horizontal component of body forces and

$$\vec{f} = f\vec{k} \qquad (2.5)$$

In (2.5) $f = 2\Omega \sin\phi$ is known as the Coriolis parameter, where ϕ stands for latitude. The control exerted by f diminishes sharply as we approach the equator.

The thermal stratification of the atmosphere is represented by the vertical gradient of entropy (s). It is convenient to express it as a frequency (N). We put

$$N^2 = \frac{g}{c_p} \frac{\partial s}{\partial z} = \frac{g}{T} \left(\frac{g}{c_p} + \frac{\partial T}{\partial z} \right) \qquad (2.6)$$

where c_p is the specific heat of air at constant pressure and T stands for temperature. The conservation of entropy is expressed by the first law of thermodynamics. It is convenient to do this in terms of the 'potential' temperature (θ) of a parcel of air. This denotes a hypothetical temperature which the parcel will acquire if it was brought adiabatically to a standard pressure (p_o). We have

$$\theta = \exp(s/c_p) \qquad (2.7)$$

whence

$$s = c_p \ln \theta \qquad (2.8)$$

The first law of thermodynamics is

$$\frac{Ds}{Dt} = \frac{D}{Dt}(\ln \theta) = \frac{Q}{c_p T} \qquad (2.9)$$

where Q is the rate of addition of heat per unit mass.

A different way of expressing (2.9) is to consider another expression for θ,

$$\theta = T \left(p_o/p \right)^k \qquad (2.10)$$

where $k = R/C_p$ and R is the gas constant. Logarithmic

differentiation of (2.9) and the assumption of hydrostatic balance yields

$$\left(\frac{\partial}{\partial t} + \vec{V}_h \cdot \nabla_p\right)\left(\frac{\partial \phi}{\partial p}\right) - \left(\frac{1}{\theta}\frac{\partial}{\partial p}\ln\bar{\theta}\right)\omega = -\frac{Q}{c_p T} \quad (2.11)$$

where $\phi = gz$

is referred to as the geopotential of an air parcel; in (2.11) we have used pressure as a vertical coordinate for which the vertical components of motion is $\omega = \frac{Dp}{Dt}$. The coefficient of ω may be expressed in different ways. It can be shown, for example, that it is equal to

$$\left(\frac{RT}{g}\right)^2 \times \frac{N^2}{p^2} .$$

Finally, the conservation of mass is expressed by the equation of continuity

$$\frac{1}{\rho}\frac{d\rho}{dt} + \nabla \cdot \vec{V} = 0 \quad (2.12)$$

If pressure is used as a vertical coordinate, the equation of continuity takes the convenient form

$$\nabla_p \cdot \vec{V}_h + \frac{\partial \omega}{\partial p} = 0 \quad (2.13)$$

The subscript p denotes differentiation on a surface of constant pressure.

To the three component equations of (2.1), along with 2.9 (or 2.11) and 2.12 (or 2.13), we add the gas law

$$p = RPT \quad (2.14)$$

to obtain a system of six equations for the six unknowns: three components of V, p, ρ and T.

The aim of numerical weather prediction is to determine the response of the atmosphere, on different scales of length and time, when it is forced by body forces represented by Q and $\vec{F}$. The major difficulties

are

- the system is nonlinear
- observational errors make it difficult to specify initial conditions accurately
- the earth's uneven terrain and the complex nature of the upper atmosphere lead to difficulties in upper and lower boundary conditions.

4. NON DIMENSIONAL NUMBERS

Further insight on the scale of atmospheric motion is gained by considering dimensions.

Let L, D represent the characteristic horizontal and vertical dimensions of a meteorological system. L is usually taken to be 1/4 the wavelength of a disturbance. The time scale (T) of the system is, similarly, 1/4 its period. The characteristic speed of propagation is represented by U. Instead of D, it is often convenient to use a scale height (H). This is the altitude at which the pressure or density of an isothermal atmosphere is reduced to 1/e of its surface value.

We put

$$H = \frac{R\bar{T}}{g} \quad (3.1)$$

where $\bar{T}$ is the mean temperature of an isothermal atmosphere. It is approximately 10 km in the tropics.

The characteristic dimensions may be combined to form non-dimensional numbers. Meteorological systems are frequently scaled by the following numbers.

(i) Rossby Number (R_o)

This is defined as the ratio of the inertial and Coriolis force. We have

$$R_o = \frac{U}{fL} = \text{Inertial force } (U/L) \quad (3.2)$$

$$\div \text{ Coriolis force } (f)$$

R_o is about 0.1 for mid-latitude systems, but becomes increasingly large as we approach the equator.

(ii) Richardson Number (R_i)

This measures the thermal stratification of the atmosphere. We have

$$R_i = g\left(D/U\right)^2 \frac{\partial}{\partial z} \ln \bar{\theta} \quad (3.3)$$

where $\bar{\theta}$ is the mean potential temperature of the atmosphere. Noting that

$$N^2 = g \frac{\partial}{\partial z} \ln \bar{\theta}$$

We have

$$R_i = N^2 \times \left(D/U\right)^2 \quad (3.4)$$

It is interesting to note that $R_o^2 R_i$ forms another non-dimensional number defined by

$$R_o^2 R_i = \frac{N^2}{f^2} \times \left(D/L\right)^2 \quad (3.5)$$

For typical atmospheric temperature gradients N is much larger than f. While N^2 is about $10^{-4}\ s^{-2}$, f^2 $10^{-9}\ s^{-2}$; consequently, $R_o^2 R_i$ is large unless D/L is very small.

(iii) Froude Number (F).

The Froude Number measures the significance of gravity. It is defined by

$$F = U/(gH)^{1/2} \quad (3.6)$$

In some cases, a rotational Froude Number (F_r) is used. It is

$$F_r = fL/(gH)^{1/2}$$

(iv) Reynolds Number (R_e)

This expresses the ratio of inertia and visions forces. It is

$$Re = UL/\nu \quad (3.7)$$

where ν is the coefficient of kinematic viscosity. R_e is of the order of 10^{13} for atmospheric systems if, $L = 500\,km$, $U = 10\,ms^{-1}$ and $\nu = 10^{-5}\,m^2 s^{-1}$.

(v) Planetary Scale Number (L/a).

The linear dimension of a meteorological disturbance (L) compared to the earth's radius (a) provides a Planetary Scale Number.

As the Coriolis parameter (f) is very small near the equator, it is often expanded in a Taylor series

$$f = f_o + \left(\frac{df}{dy}\right)_o y + \cdots \quad (3.8)$$

where the subscript 0 refers to values at the equator. Putting

$$\beta = \left(\frac{df}{dy}\right)_o = \frac{2\Omega \cos \phi_o}{a} \quad (3.9)$$

We have

$$f = f_o + \beta\left(L/a\right) y_* + \cdots$$

where

$$y_* = y/L .$$

Expansion of f in this manner is referred to as the beta plane approximation. It allows retention of the spherical geometry of the earth for small distances, without losing the simplicity of cartesian coordinates.

5. DIFFERENCES BETWEEN TROPICS AND MID-LATITUDES.

The different non-dimensional numbers point to different scaling techniques, when we compare motion in

mid-latitudes with the tropics. A few typical values are presented in Table 1.

Table 1.

Scale Features

Number	Mid-latitudes	Tropics
R_o	0.10	1.0
R_i	10^2	10^2
$R_o^2 R_i$	1.0	10^2
F_r	0.3	0.03
L/a	0.1	0.1

The above values are relevant for large scale motion, The characteristic values for this scale of motion are

$L \sim 10^6$ m

$N^2 \sim 10^{-4}$ S^{-2}

$U \sim 10$ mS^{-1}

$H \sim 10^4$ m

$f \sim 10^{-4}$ S^{-1} for mid-latitudes and

10^{-5} S^{-1} for tropics.

6. VORTICITY AND DIVERGENCE

In the year 1938, the celebrated Swedish meteorologist, C.G. Rossby, put forward the suggestion that meteorological systems in the mid-latitudes move in a manner which conserves their spin, or the vertical component of their

vorticity. This is

$$\zeta = \vec{k} \cdot \nabla \times \vec{v} \qquad (4.1)$$

This simple concept formed the basis for numerical weather prediction in the early years.

Another variable, which is frequently referred to in atmospheric dynamics, is the divergence of the velocity vector.

$$\nabla \cdot \vec{v} = D \qquad (4.2)$$

As we shall see later, in mid-latitudes the vorticity is an order of magnitude larger than divergence (D). This enables us to treat large-scale motion in the mid-latitudes as being quasi-geostrophic in nature. Geostrophy implies a balance between the forces due to pressure gradient and the earth's rotation. The geostrophic wind is approximately non-divergent. Consequently, it is often possible to express the wind vector as the gradient of a stream function. This advantage is no longer available in the tropics, because f is small and the geostrophic balance is no longer valid. It is also not always a case of in low latitudes. Consequently, tropical meteorologists have tried to derive a streamfunction in which the constraint is that the rate of change of divergence (D) is small, instead of neglecting D altogether.

The ratio $\frac{H}{L} = \frac{f}{N}$

often occurs in the theory of uniformly rotating stratified fluids. This measures the depth of the fluid response (H) to a disturbance of horizontal length (L). Rossby (1938) defines the number $\frac{NH}{f}$ as a radius of deformation.

It measures the length of fluid 'deformed' or disturbed by a given scale (L) of the perturbation. As f is small in the tropics and N is large, it is observed that the upper and lower troposphere are decoupled from each other for large scale meteorological systems. In the tropics the link is provided by the cumulative effect of small scale convection. Models for the tropics are now endeavouring to consider this aspect in detail.

Another property of the atmosphere that is relevant here is referred to as its potential vorticity. This is the ratio of the vorticity of the air and the earth's spin divided by the atmospheric depth (h). The conservation of potential vorticity is expressed by

$$\frac{d}{dt}\left(\frac{\zeta+f}{h}\right) = 0 \qquad (4.3)$$

This theorem which was derived by Ertel in 1942 is another expression for the conservation of angular momentum, because the angular velocity of a fluid column is $(\zeta+f)/2$. The name 'potential vorticity' is a little unfortunate, because expressions are derived which are, in an approximate sense, a combination of absolute vorticity $(\zeta+f)$ and the thermal stratification of the fluid. As the depth (h) is related, albeit loosely, to the vertical gradient of potential temperature, this is referred to as the potential vorticity. These aspects have been discussed in more detail by Haltiner and Williams (1980) and Phillips (1973).

REFERENCES

Bjerkness, V. 1904 Das problem von der Wettervorhersage, Meteor. Z., 21, 1-7.

Charney, J.G., R. Fjortoft, and J. Von Neumann 1950 Numerical integrations of the barotropic vorticity equation, Tellus, 2, 227-254.

Haltiner, G.J. and R.T. Williams 1980 Numerical prediction and dynamic meteorology, Second Edition, John Wiley & Sons, 477, pp.

Phillips, N.A. 1973 Principles of large scale numerical weather prediction, in Dynamic Meteorology, Ed. P. Morel, D. Reidel Publishing Co., 1-96 pp.

Richardson, L.F. 1922 Weather prediction by numerical process, Camb. Univ. Press, 236 pp.

Rossby, C.G. 1938 On the mutual adjustment of pressure and velocity distribution in certain simple current systems, J. Marine. Res, Sears Foundation, 239-263.

LECTURE IV

1. COMPUTATIONAL DESIGN

(a) Finite differences.

Finite differences have been most widely used to replace derivatives in the governing equations. This approximation is made at a discrete set of points in space and time. This is referred to as a grid. Cartesian and Spherical coordinates are both used.

Replacement of derivatives by finite differences increases the order of the original equation. This gives rise to an additional computational mode, apart from the physical mode which the mathematical equation seeks to describe. Computational modes lead to an exponential amplification of the numerical solution. Computational instability may be woided by imposing the constraint

$$\left| C \frac{\Delta t}{\Delta x} \right| \leq 1 \qquad (1.1)$$

on the numerical scheme. C is the phase speed of the fastest growing wave and $\Delta t, \Delta x$ are increments in space and time. This is known as the Courant-Friedrichs-Levy (CFL) criterion.

Numerical schemes, which seek to simulate non-linear systems, should satisfy a number of invariants. For meteorological systems quadratic invariants, such as, the total kinetic energy and the enstrophy (square of vorticity) need to be preserved.

Finite difference schemes which satisfy these conservation principles have been developed by Arakawa (1966). This is illustrated by a simple prediction equation

$$\frac{\partial \zeta}{\partial t} = J(\psi, \zeta) \qquad (1.2)$$

where ζ is the vertical component of vorticity and ψ is a stream function to represent the non divergent component of the wind vector. J is the Jocobian operator which may be expressed in three different ways:

$$\begin{aligned} J &= \psi_x \zeta_y - \psi_y \zeta_x \\ &= (\psi \zeta_y)_x - (\psi \zeta_x)_y \\ &= (\zeta \psi_x)_y - (\zeta \psi_y)_x \end{aligned} \qquad 1.3\cdot(a,b,c)$$

These expressions can be represented on a nine point stencil (fig.1).

Fig. 1

Nine point stencil

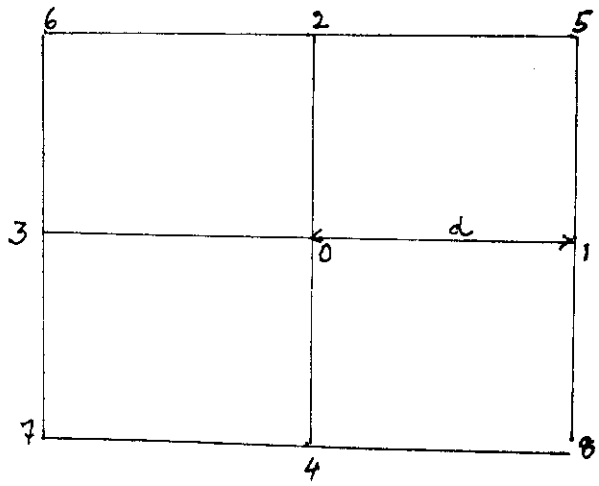

The equivalents of (1.3 a,b,c) are:

$$J^{++} = \frac{1}{4d^2}\left[(\psi_1-\psi_3)(\zeta_2-\zeta_4) - (\psi_2-\psi_4)(\zeta_1-\zeta_3)\right]$$

$$J^{+x} = \frac{1}{4d^2}\left[\psi_1(\zeta_5-\zeta_8) - \psi_3(\zeta_6-\zeta_7) - \psi_2(\zeta_5-\zeta_6) + \psi_4(\zeta_8-\zeta_7)\right]$$

$$J^{x+} = \frac{1}{4d^2}\left[\zeta_2(\psi_5-\psi_6) - \zeta_4(\psi_8-\psi_7) - \zeta_1(\psi_5-\psi_8) + \zeta_3(\psi_6-\psi_7)\right]$$

By a little algebra involving computation of $\zeta_0 J_0^{++}$, $\zeta_1 J_1^{++}$ etc it can be shown that only the average of J^{++}, J^{+x} and J^{x+} conserves both enstrophy and kinetic energy (Haltiner and Williams, 1980).

Non-linear systems are also subject to aliasing errors. When waves, which are too short to be resolved by a given set of grid points, interact they lead to an unrealistic growth of energy. It is possible to exercise some control over aliasing errors by utilising a filter. The inclusion of an artificial diffusing term has been employed, but none of these methods are completely satisfactory.

(b) Variable and nested grids

To study the planetary aspects of a meteorological phenomenon, such as, the variability of climate, it is necessary to use general circulation models (GCM). This is expensive in terms of manpower and money. For countries which do not have access to large computers, a possible strategy might be to employ a model with a variable grid. This has high resolution over the region of interest, with coarse resolution elsewhere. This is achieved by using stretched coordinates. A GCM of this type has been recently developed in India, in collaboration with France

(Sharma and Sadourny, 1984).

Another strategy that has been employed utilizes limited area models for problems of regional interest (Raymond and Kuo, 1984; Okamura, 1975). Such models are also useful for simulating small scale atmospheric phenomena. The central problem in such models is concerned with lateral boundary conditions. If the boundary conditions are reflective, that is, the boundaries are rigid walls which reflect waves propagating out of the region, the results are not satisfactory beyond a few ways of integration. The faster intertial-gravity waves soon spoil the solution after repeated reflection, even if they are filtered out as far as possible before integration is commenced.

Open boundary conditions, which permit the entry and exit of flow patterns are preferable. This is achieved by a Sommerfeld radiation condition at the boundary:

$$\frac{\partial \phi}{\partial t} + c\frac{\partial \phi}{\partial n} = 0 \qquad (1.4)$$

where ϕ is a dependent variable, c the phase velocity, t is time and n stands for coordinate normal to the boundary. This type of boundary condition enables one to determine whether energy is entering or leaving the region. It was first used for meteorological problems by Orlanski (1976). Unfortunately, determination of the phase speed is not easy because it is not known in advance what waves are likely to be generated. As we have

...en earlier, at low latitudes it is difficult to separate the Rossby and intertia-gravity modes. The radiation condition has not been much used in low latitudes. Raymond and Kuo (1984) find some improvement if the phase velocity c in (1.4) is a combined expression for the phase velocity in all three directions (ox, oy and oz) in place of the phase velocity in only one direction.

Lateral boundary conditions are also important for nested grid models. These models use the output from a coarse grid as the boundary conditions for a fine mesh of higher resolution over a limited area. But, this provides only one-way interaction between the coarse and fine mesh. In order to have two way interaction, the fine mesh solution must influence the coarse mesh as well, this means that the integrations for both regions must be integrated simultaneously. Several techniques for doing this are now being investigated.

(c) Upper and lower boundary conditions.

Most models assume that the vertical component of velocity vanishes at the top of the atmosphere For models that seek to simulate the upper atmosphere this condition is not realistic. The radiation condition which permits upward flow of energy, is more realistic. This is especially important for flow patterns forced by large orographic barriers.

The lower boundary condition cannot be applied

at sea level if the mountains are very high. To apply the correct pressure would create computational instability, because if H be the height of a mountain the vertical component of motion as the air flows past it is

$$\omega = \vec{V} \cdot \nabla H \qquad (1.5)$$

and very large values of ω are generated by sharp changes in the gradient of H. Several devices are used to get over this difficulty, and none of them are completely satisfactory.

A sigma coordinate system is often employed. This expresses the vertical coordinate as a function of pressure by

$$\sigma = p/p_s \qquad (1.6)$$

where p_s is the surface pressure. The lower boundary this becomes a material surface, which takes care of the gradients of H. This avoids application of the lower boundary at different pressures, but raises another difficulty. The pressure gradient force is now expressed by

$$\nabla_p \Phi = \nabla_\sigma \Phi + \frac{RT}{p_s} \nabla p_s \qquad (1.7)$$

where the subscripts p, σ refer to derivatives on surface of constant pressure and sigma respectively. Φ is geopotential, R is the gas constant and T stands for temperature. The two terms on the right of (1.7) are large and of opposite sign; consequently, the pressure gradient is a small difference between two large terms of opposite sign. Experiments suggest that if deviations are considered from mean values for a standard atmosphere, then the magnitude of the two

terms on the right of (1.7) are reduced. This reduces the possibility of error. This problem is of considerable importance for inclusion of high topographic barriers, such as, the Himalayas in numerical models.

(d) Minimising truncation errors for different thermal stratifications.

A problem which is attracting much research interest is concerned with the thermal stratification that will minimize vertical truncation errors. In the vicinity of steep mountains, it is of some advantage to remove an average geopotential from the total geopotential and to use the residual as a dependent variable. There are several choices for defining an average. Geopotentials corresponding to an isothermal or an isentropic atmosphere are examples of different options. The best choice will be one which suppresses the intertia-gravity waves.

2. INITIALISATION.

Mention was made earlier of the need for filtering out the meteorological noise before commencing integration. This process is referred to as initialization. In earlier models, this was achieved by invoking geostrophic balance in the initial state. Another device was to remove the time dependence of a small divergent component of the wind vector. This led to a "balance" equation which provides a better balance between the wind vector and the pressure gradient, because some of the wind divergence was included. Geostrophic balance precludes any divergence.

Although these methods, which are essentially linear filters, remove a good part of gravity modes, there still remains a residue - because of non-linear interactions - at the start of integration. It was proposed by Machenhauer (1976) that this residue could be counterbalanced by introducing a correction. The governing equations for atmospheric motion may be writtern symbolically as

$$\dot{\underline{X}} = i\underline{L}\underline{X} + \epsilon N(X) \qquad (2.1)$$

where $i\underline{L}\underline{X}$ are the linear terms and the non-linear terms are N(x). ϵ represents a small parameter, such as the Rossby number for mid-latitude systems.

Let

$$\underline{X} = R\underline{X} + G\underline{X} \qquad (2.2)$$

where R and G stand for the Rossby and gravitational modes, Non-linear normal mode initialization imposes the condition

$$G\dot{X} = 0 \qquad (2.3)$$

where

$$GX = i\epsilon (LG)^{-1} G N(X) \qquad (2.4)$$

This technique has not yet been used in limited area models, or in the tropics where the distinction between R and G is to some extent blurred.

3. SPECTRAL MODELS

In alternate approach to grid point models is to express the dependent variables as orthogonal functions. The prediction equations then become ordinary differential equations for the coefficients of the series that is employed.

Let the stream function ψ be expressed by

$$\frac{\partial \psi}{\partial t} = F(\psi) \qquad (3.1)$$

The stream function may be expressed by a series

$$\psi(x,t) = \sum_{j=1}^{N} A_j(t)\, b_j(x) \qquad (3.2)$$

Inserting (3.2) in (3.1) provides N equations for the N unknowns $\frac{dA_j}{dt}$. The system is simplified if the basis functions are orthogonal to each other, and are normalised, so that

$$\int b_j b_k \, dx = 1 \qquad (3.3)$$

if j = k, but vanishes otherwise.

For a fuller account of spectral methods a reference may be made to Kasahara (1977). At present spectral methods have not been much used in the tropics, because the non-linear interactions need much computation time. Attempts to speed up computation by the use of transforms are in progress.

4. MULTILEVEL MODELS

The problem of vertical discretization arises in multilevel models. The usual procedure is to divide the atmosphere into a number of discrete layers. Expressions for the conservation of vorticity and the first law of

thermodynamics are then used in different layers, so as to match the solution at the interface between adjacent layers. The system of equations is then solved by three dimensional relaxation. The procedure is best illustrated by a simple two layer model.

The atmosphere is divided into 4 discrete layers, in which the four surfaces (n) are numbered 0 to 4 as shown in the following figure.

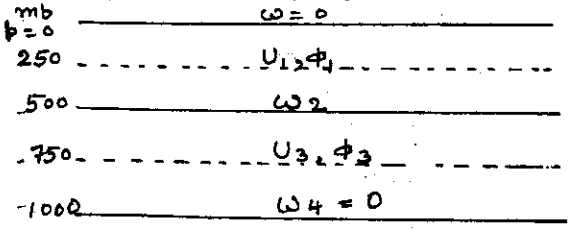

Assume we have flat ground so that $\omega = 0$ at p = 0 and 1000 mb. Further, let U_1, Φ_1 and U_3, Φ_3 represent the zonal velocity and geopotential at levels 1 and 3. Applying finite differences for vertical derivatives we have

$$\left(\frac{\partial \omega}{\partial p}\right)_1 = \frac{\omega_2 - \omega_0}{\Delta p}, \quad \left(\frac{\partial \omega}{\partial p}\right)_3 = \frac{\omega_4 - \omega_2}{\Delta p}$$

Recall that the conservation of vorticity and the first law of thermodynamics are

$$\left(\frac{\partial}{\partial t} + U\frac{\partial}{\partial x}\right)(\zeta + f) - f\frac{\partial \omega}{\partial p} = 0 \qquad (4.1)$$

$$\left(\frac{\partial}{\partial t} + U\frac{\partial}{\partial x}\right)\left(\frac{\partial \Phi}{\partial p}\right) + \Gamma\omega = 0 \qquad (4.2)$$

where $\Gamma = -\frac{1}{\rho}\frac{\partial}{\partial p}\ln\bar{\theta}$ represents the static stability parameter. Replacing the vertical derivatives by finite differences, the conservation of vorticity at

levels 1 and 2 provide

$$\left(\frac{\partial}{\partial t} + u_1 \frac{\partial}{\partial x}\right)\zeta_1 + f^2 \frac{\omega_2}{\Delta p} = 0 \qquad (4.3)$$

$$\left(\frac{\partial}{\partial t} + u_3 \frac{\partial}{\partial x}\right)\zeta_3 - f^2 \frac{\omega_2}{\Delta p} = 0 \qquad (4.4)$$

Similarly, applying the first law of thermodynamics at level 2 we get

$$\left(\frac{\partial}{\partial t} + \bar{u} \frac{\partial}{\partial x}\right)(\phi_1 - \phi_3) + (\Gamma \Delta p)\omega_2 = 0 \qquad (4.5)$$

where $\bar{u} = \frac{1}{2}(u_1 + u_3)$

Equations (4.3), (4.4) and (4.5) provide 3 equations for the unknowns, ζ_1, ζ_3, ω_2. Note that adding (4.3) to (4.4) we get a prognostic equations for the average vorticity between levels 1 and 3. Similarly, if (4.4) is subtracted from (4.3) we get a prognostic equation for the thickness $(\phi_1 - \phi_3)$ between the two levels. The forcing terms in this simple geostrophic and adiabatic model are represented by the advection of vorticity and temperature.

Further algebraic manipuation, shows that available potential energy of the atmosphere is converted to the kinetic energy of motion if the warmer air $((\phi_1 - \phi_3) > 0)$ is rising and cooler air $((\phi_1 - \phi_3) < 0)$ is sinking. This is an interesting result which has many ramifications in atmospheric physics.

5. PRACTICAL APPLICATIONS

Towards the end of 1982, twenty four hour upper wind precasts were commenced on real time by the European

Centre for Medium Range Weather Forecasts (ECMWF). This is located at Bracknell in the United Kingdom, and its forecasts are transmitted on global telecommunication links. A 5-layer limited region model that was developed in India was used to compare forecasts of upper winds over the Indian region. The results are presented in Table 1.

Table 1.

Twenty four hour upper wind forecasts.

Average root mean square error of vector winds (in knots) from August 1982 to January 1983.

Pressure (mb)	850		200	
Month	ECMWF	India	ECMWF	India
August	14.4	16.0	18.5	20.3
September	11.0	14.5	16.8	20.8
October	9.3	11.9	18.5	21.8
November	10.6	13.8	23.5	25.1
December	11.2	13.8	23.8	27.5
January	11.3	13.6	29.1	36.5

The performance of the ECMWF is better because it has much greater vertical resolution and more in-built physics, but the comparison shows that encourging results can be achieved with limited area models on a medium-size computer.

REFERENCES

Machenhaner, B.	1977	On the dynamics of gravity oscillations in a shallow water model, with application to normal mode initialization, Contrib. Atmos. Phys. 50, 253-271.
Orlanski, I.	1976	A simple boundary condition for unbounded hyperbolic flows, J. Comp. Physics, 21, 251-269.
Okamura, Y.	1975	Computational design of a limited area prediction model, J. Met. Soc., Japan, 53, 3, 175-188.
Raymond, W.H. and H.L. Kuo.	1984	A radiation boundary condition for multi-dimensional flows, Quart. J.R. Met. Soc., 110, 464, 535-552.
Sadourny, R. and O.P. Sharma.	1984	Monsoon prediction using a general circulation model with horizontally varying mesh, Proc. Symposium on Climate and its Variability,

(Contd.)

Sadourny, R. and O.P. Sharma.	Centre for Atmospheric Sciences, India Institute of Technology, New Delhi, 110016, India, 280-301.

NUMERICAL MODELS - P.K. Das

LECTURE V

1. PARAMETERIZATION OF SOLAR RADIATION

Numerical models consider solar radiation in two parts: one for shortwave incoming solar radiation (o.15 to 2.0 microns) and another for long wave terrestrial radiation (4 to 80 microns).

The depletion of incoming solar radiation is considered under three ranges (table 1).

Table 1.

Depletion of Solar radiation

Wavelength (microns)	Atmospheric response.
Less than 0.3	Almost completely absorbed by oxygen and ozone in the upper atmosphere.
0.3 - 0.7	Depleted by scattering.
0.7 - 2.0	Attenuated by water vapour absorption. CO_2 absorption is small.

There are several ways of parameterizing absorption and scattering and different models adopt different procedures. The aim will be to illustrate physical

principles.

Wavelengths less than 0.3μ are usually neglected, because in this range solar energy does not reach the lower stratosphere or the troposphere. In any event the energy content of this region is small.

The undepleted flux of solar radiation reaching the top of the atmosphere is expressed by a Cosine law

$$F = S \cos\theta \qquad (1.1)$$

where S is the intensity of solar radiation (I) weighted by the ratio of the sun's radius (a) and its mean distance from the earth (r). We have

$$S = \pi\left(\frac{a}{r}\right)^2 I \qquad (1.2)$$

The sun's zenith angle is θ which depends on latitutde, the hour angle and the sun's declination. Values of these variables are available in an almanac for any time of the year.

As scattering and absorption by water vapour are two important processes that deplete solar radiation, the incident beam at the top of the atmosphere is divided into two parts, a scattered part (F_s) and a part that is absorbed (F_a). We put

$$F_s = 0.651\ F \qquad (1.3, a,b).$$

$$F_a = 0.349\ F$$

2. DEPLETION BY SCATTERING

Half the scattered radiation is assumed to be directed upwards while the other half is directed downwards.

The upward beam is lost to space. This is typical of Rayleigh scattering, which is inversely proportional to the fourth power of wavelength. Rayleigh scattering is true for particles whose diameters are small compared to the wavelength of the incident radiation. When the diameters of scattering particles exceed the wavelength of incident radiation, the downward scattered beam begins to predominate. Non isotropic scattering is usually ignored in numerical models, but this could be important for an atmosphere with a heavy dust load.

The albedo, is the reflective power of the atmosphere. The albedo of a cloudless atmosphere is

$$a_o = 0.085 - 0.247 \log_{10}\left(\frac{p_s}{1000}\cos\theta\right) \quad (2.1)$$

where p_s is the surface pressure. The amount of scattered radiation reaching the ground is $F_s(1-a_o)$. Let a_s represent the albedo of the earth's surface. Hence, the fractional reflection from the surface is

$$[F_s(1-a_o)]a_s$$

Of this amount, a fraction a_o is reflected back again to earth. Proceeding in this manner, the solar radiation reaching the ground is the sum of scattered fractions, that is,

$$1 + a_o a_s + a_o^2 a_s^2 + \cdots = \frac{1}{1 - a_o a_s} \quad (2.2)$$

Finally, the scattered radiation reaching the ground is

$$F_s \frac{(1-a_o)}{(1-a_o a_s)} \quad (2.3)$$

If there is a single cloud layer, it can be shown

that a_o must be replaced by a_c, where

$$a_c = 1 - \frac{(1-R_c)}{1-a_o a_s} \quad (2.4)$$

where R_c is the reflectivity of the cloud layer. Similar expressions may be derived for two contiguous cloud layers or two separated cloud layers.

3. DEPLETION BY WATER VAPOUR ABSORPTION

Based on laboratory data, the absorption by water vapour (A) is

$$A(u) = 0.279(u\sec\theta)^{0.303} \quad (3.1)$$

where u is the optical depth of the atmosphere. It is usually expressed by

$$u(p) = \frac{1}{g}\int_0^p q\,(p/p_s)^{0.95}\,(T_s/T)^{0.5}\,dp \quad (3.2$$

where q is the specific humidity of air.

The direct solar radiation reaching a reference level i is then,

$$F_A\left[1 - A(u\sec\theta)\right] \quad (3.3)$$

where only the absorbed part F(A) is attenuated,

To estimate the net downward flux of direct solar radiation at a given reference level (i), the amount of diffuse radiation that comes up from the earth's surface needs consideration. This is

$$F_A\left[1 - A(u_o)\right]a_s \quad (3.4)$$

where u_o is the optical depth at $p = p_s$ (equation 3.2).

Subtracting (3.4) from (3.3) gives the flux of solar radiation reaching the earth's surface from level i. And, on summing up for several reference levels we get the net flux of downward solar radiation. Some models introduce minor corrections to account for the larger path length of diffuse radiation, but they will not be discussed here.

Modifications are also introduced to take into account either a single cloud layer, or multiple cloud layers. For this purpose, the incoming solar radiation at the top of the cloud, and the upward diffuse radiation from the cloud top is calculated. Subsequently, the absorption by the cloud is computed by considering the amount of water vapour in the cloud (q in equation (3.2), and the albedo of the cloud. The details are not reproduced here, but the interested reader will find the full details in a paper by Katayama (1972).

4. TERRESTRIAL LONG WAVE RADIATION

The rate at which the atmosphere is warmed or cooled by long wave radiation is measured by the difference in upward (F) and downward (G) fluxes. The latter is often referred to as the flux divergence in the layer between Z and Z + dZ,

$$\frac{\Delta T}{\Delta t} = \left[G(z+\Delta z) - G(z) - F(z+\Delta z) + F(z)\right] \quad (4.1)$$

Most models divide the long wave radiation spectrum into a number of intervals. A representative value of atmospheric transmission is then assumed for

each interval. The principal constituents of the atmosphere which absorb long wave radiation are ozone, carbon dioxide and water vapour. In general, the atmosphere absorb long wave radiation more strongly than shortwave radiation. Absorption by water vapour around 6 and 20 microns is important for tropospheric problems.

Suitable modifications are introduced in (4.1) when clouds are present. For most practical purposes, clouds may be treated as black body radiators.

Unfortunately, the computation of transmission functions, which are needed to calculate F and G in (4.1), is not straightforward. The transmission function in a spectral interval $\Delta\lambda$ is of the form

$$\tau_{\Delta\lambda} = \frac{1}{\Delta\lambda} \int_{\Delta\lambda} \exp - \left[\int_{\Delta u} k(\lambda)\, du\right] d\lambda \quad (4.2)$$

where $k(\lambda)$ is the absorption coefficient at wavelength λ.

The water vapour spectrum in the long wavelength regions contains several hundred lines. The shape of each line is related to the absorption coefficient by

$$k(\lambda) = \frac{S}{\pi} \frac{\alpha}{(\lambda-\lambda_0)^2+\alpha^2} \quad (4.3)$$

where S is the line intensity, λ_0 is the central wave length and α is the half width of the line. Both α and u are functions of pressure. We have

$$\alpha = \alpha_0 \left(p/p_s\right) \left(T_s/T\right)^{1/2} \quad (4.4)$$

To obtain F or G, equation (4.2) has to be integrated over both u and λ. In view of the rapid fluctuations of $k(\lambda)$ with λ and α no ideal solution has yet been found. To simplify matters,

The interval $\Delta\lambda$ is so chosen that absorption lines do not overlap but, in reality, there is considerable overlap between individual lines. In early models, it used to be assumed that the spectrum was made up of individual lines that did not overlap, and α, S were constant in (4.3). When such an assumption is made analytical expressions for the transmission function may be derived in terms of Bessel functions of imaginary argument. Putting

$$x = \frac{S u}{2\pi\lambda} \qquad (4.)$$

the transmission function for large x was

$$\tau = 1 - 2\left(\frac{S u \alpha}{\Delta\lambda}\right)^{1/2} \qquad (4.5)$$

This was known as the square root law of absorption. But, as we can see from (4.4) α depends on pressure and temperature. Consequently, the square root-law is not realistic because of the wide variation in pressure and temperature over the depth of the atmosphere.

An improvement over this somewhat unsatisfactory state was made by Goody (1964) who introduced the assumption that all positions of individual lines were equally probable. The probability of a line having an intensity S is then given by

$$P(S) = \frac{1}{\bar{S}} \exp\left(-S/\bar{S}\right) \qquad (4.6)$$

where $\bar{S}$ is the mean line intensity. The advantage is that an array of lines in a given interval $(\Delta\lambda)$ may be replaced by a single line in a statistical sense. But, the transmission function still has the limitation

of a constant α.

Further analysis by Curtis (1956), showed to a large degree of accuracy, it was only necessary to consider the line width, rather than its whole shape, dependent on statistical distribution. For atmospheric problems, it was sufficient to consider all absorbing matter to be located at a pressure ($\bar{p}$) given by

$$\bar{p} = \int p(z)\rho(z)dz \Big/ \int \rho(z)dz \qquad (4.7)$$

Although the model by Curtis was published nearly two decades ago, it is still used to compute transmission functions and, finally, the rate of radiative heating or cooling. A recent example of its application is by Wehrbein and Leovy (1982) for the middle atmosphere.

5. CUMULUS PARAMETERIZATION

It is now increasingly realised that collective effect of individual cumulus clouds can influence large scale meteorological systems by the vertical transfer of heat, moisture and momentum. This is especially true of the tropics, where meteorological systems derive their energy from the latent heat released by clouds.

Cumulus clouds tend to warm and dry the atmosphere. Synoptic systems, such as, African waves, support Cumulus clouds by creating conditions that favour the growth of clouds by convergence of moisture. A form of cooperative interaction is thus set up in which (a) cumulus clouds feed energy to atmospheric

systems by the release of latent heat and (b) atmospheric waves create conditions that lead to cloud formation. This was named conditional instability of the second kind (CISK) by the late Professor J.G. Charney.

Several schemes are now available for parameterizing the effect of an ensemble of clouds. The most widely used ones are by (a) Kuo (1965 , 1975) and (b) Arakawa and Schubert (1974). We wish to discuss the physical principles of each.

6. KUO'S SCHEME

The numerical model will generate cumulus clouds if the atmosphere is unstable, and there is convergence of moisture accompanied by ascending motion. Instability is determined by the prevailing verzical gradient of temperature (called lapse rate in meteorology).

Let,

M_t = Mositure convergence produced by large scale flow and evaporation from the surface.

$(1-b)\ M_t$ = Rate of precipitation

bM_t = Rate at which the atmosphere is moistened before condensation begins.

where b represents the fraction of M_t which is stored in the atmosphere.

The value of M_t is calculated by

$$M_t = -\frac{1}{g}\int_{p_t}^{p_b} \nabla\cdot(q\vec{v})\,dp + C_D \rho_s V_s (q_s - q_a) \quad (5.1)$$

The first term is the convergence of moisture, while the second term on the right denotes evaporation from the earth's surface. q_s is the saturation mixing

ratio over the surface, and q_a is the mixing ratio of the overlying air. ρ_o , C_D represent the density of surface air and an exchange coefficient for transfer of water vapour.

The cumulus cloud is assumed to have a temperature excess $(T_c - T)$ .and a moisture excess $(q_c - q)$ over the environment. q_c is the saturation mixing ratio at the temperature of the cloud (T_c). The storage fraction (b) is given by

$$b = \int_{p_t}^{p_b} (q_c - q)\,dp \;\div\; \int_{p_t}^{p_b} \left[\frac{c_p}{L}(T_c - T) + (q_c - q)\right] dp \quad (5.2)$$

p_t and p_b represent the top and bottom of a cloud.

It follows from (5.2) that if the air is dry, b is large and most of the moisture is used up to moisten the atmosphere.

The [illegible] heating rate due to latent heat release is

$$\int_{z_b}^{z_t} \epsilon\, dz = (1-b)\, L\, M_t \quad (5.3)$$

where L is the latent heat of condensation and ϵ is the rate of heating per unit mass. An average heating rate may be defined from (5.3) by,

$$\overline{\epsilon} = \frac{1}{z_t - z_b}\int_{z_b}^{z_t} \epsilon\, dz \quad (5.4)$$

The vertical distribution of heating is, approximately, $\overline{\epsilon}$ weighted by a vertical distribution function N(p). As the environment and clouds do not interact, N(p) may be taken proportional to the temperature excess $(T_c - T)$. We put

$$N(p) = \left[(T_c - T)(p_b - p_t)\right] \div \int_{p_t}^{p_b} (T_c - T)\,dp \quad (5.5)$$

Kuo's scheme has the advantage of simplicity, but it is more oriented towards cloud ensembles. Individual clouds do not figure in this scheme.

7. ARAKAWA AND SCHUBERT MODEL

Unlike Kuo's model, Arakawa and Schubert (1974) consider each individual cloud in a cloud ensembler Each cloud is identified by its rate of entrainment which, in turn, is determined by the altitude of the clo cloud top. In this manner, the clouds interact with the environment, a feature which was absent in Kuo's model. The model assumes that whatever a cloud gains through entrainment is shed by detrainment at the cloud top.

Clouds are also identified by the kinetic energy acquired by the force of buoyancy.

We have

$$\frac{d}{dt}\left(\tfrac{1}{2}\omega^2\right) = g\omega\left(\frac{T_c - T}{T}\right) \qquad (8.1)$$

where ω is the vertical velocity of air within a cloud, and $(T_c - \bar{T})$ is the cloud's temperature excess. This kinetic energy is expressed in terms of a quantity $A(z,\lambda)$ which depends on the altitude (z) and the rate of entrainment (λ). $A(z,\lambda)$ is called the cloud work function.

The model then postulates a state of equilibrium between clouds and their environment so that

$$\frac{dA(\lambda,z)}{dt} \simeq 0 \qquad (8.2)$$

This equilibrium is achieved by interaction between

the clouds and their environment. Broadly speaking, we may imagine the work function of clouds to change negatively with time, i.e, $\left(\frac{dA}{dt}\right)_{cu} < 0$, because they tend to stabilize the atmosphere by generating subsidence and drying of the clear region between adjacent clouds. On the other hand, the environment permits growth of clouds, whence $\left(\frac{dA}{dt}\right)_{ENV} > 0$.

The work function of cumulus clouds is omputed by the impact of each cloud on others. The mathematical formulation, which will not be described here, involves the solution of an integral equation by numerical methods. The work function of the environment is evaluated from budgets of water vapour and temperature.

The model is only valid when the time scale of large scale systems is much larger than the evolution time of cumulus clouds. The former is usually of the order of a few days, while the latter is only a few hours.

Arakawa and Schubert's model has been applied with considerable scuccess to several problems of atmopsheric dynamics. Full details of its application to the atmopshere will be found in papers by Lord and his collaborators (1980, 1982). An application to monsoons over India has been described by Ramanathan (1981) Another interesting application was by Shukla (1981) who included cumulus parameterization in instability analysis.

Its application to African waves would be interesting. Cumulus parameterization for monsoonal circulations will be described in the next chapter.

REFERENCES

Arakawa, A. and W.H. Schubert. 1974 Interaction of a cloud ensemble with the large scale environment, Pt. I, J. Atmos. Sci., 31, 674-701.

Curtis, A.R. 1956 The computation of radiation heating rates in the atmosphere, Proc. Roy. Soc., London, A 236 156-159.

- and R.M. Goody. 1956 Thermal radiation in the upper atmosphere, Proc. Roy. Sco., London, A 236, 193-206.

Goody, R.M. 1964 Atmospheric Radiation I, Oxford Univ. Press, 436 pp.

(contd.)

Katayama, A. 1966 On the radiation budget of the troposphere over the northern hemisphere (I), J. Met. Soc. Japan, SII, 44, 381-401.

Kuo, H.L. 1965 On the formation and intensification of tropical cyclones by Cumulus convection, J. Atmos. Sci., 22, 40-63.

- 1974 Further studies on parameterization of Cu. convection, J. Atmos. Sci., 31, 1232-1240.

Lord, S.J. and A. Arakawa. 1980 Interaction of a Cu. cloud ensemble with the large scale environment, Pt. II, J. Amos. Sci, 37, 2677-2692.

Lord, S.J. 1982 Ibid, Pt. III, 39, 88-103.

Lord, S.J., W.C. Chao and A. Arakawa. 1982 Ibid, Pt. IV, 39, 104-113.

Ramanathan, Y. 1981 Determination of cloud

(Contd.)

cluster properties
from Monsoon 77 data,
Monsoon Dynamics,
Camb. Univ. Press, Ed.
Str James Lighthill
and R.P. Pearce, 269-286.

Shukla, J. 1978 CISK, barotropic-
baroclinic instability
and the growth of a
monsoon depression, of
J. Atmos. Soc., 35,
495-508.

Wehrbein, W.M.
and
C.B. Leovy 1982 An accurate radiative
heating and cooling
algorithm for use in a
dynamical model of the
middle atmosphere,
J. Atmos. Soc., 39,
1532-1544.